ChemPubSoc Europe

DOI: 10.1002/celc.201600081

CHEMELECTROCHEM Communications

New Evidence of LiO_2 Dismutation in Lithium–Air Battery Cathodes

Maria del Pozo, Walter R. Torres, Santiago E. Herrera, and Ernesto Julio Calvo*[a]

The dismutation of electrochemically generated soluble lithium superoxide with the formation of a lithium peroxide deposit on Au has been studied by addition of lithium ions and following the mass uptake detected by the electrochemical quartz crystal microbalance at the open-circuit potential and the surface morphology evolution by using atomic force microscopy.

The increasing energy requirements of society in recent years has prompted a large number of studies related to energy storage and sustainable technologies. In this context, rechargeable Li–O_2 batteries appear as a promising alternative and are conceived primarily for automotive applications, owing to their high theoretical energy density over lithium-ion batteries.[1] In nonaqueous Li–O_2 batteries, the discharge process is the oxygen reduction reaction (ORR) at the cathode in lithium electrolyte, forming insoluble Li_2O_2 as the final product.[2] As demonstrated by Ogasawara et al. by using X-ray diffraction,[3] the recharge process is the oxidation of peroxide, evolving O_2 and Li^+ in solution (oxygen evolution reaction, OER). The battery success will depend on the reversibility of these two processes during an extended number of cycles. The electrode kinetics of the ORR in lithium–air battery cathodes strongly depends on the solvent, electrolyte, and electrode material.[4]

Two different mechanisms for the ORR in Li^+-containing nonaqueous solvents have recently been proposed,[1b,4b,5] depending on the growth of Li_2O_2 at the cathode surface, that is, surface reaction or solution-phase reaction, as compared in Scheme 1. In the surface mechanism, two adsorbed LiO_2 molecules disproportionate at the electrode surface or undergo two sequential one-electron transfer steps, whereas the solution-phase mechanism requires dismutation of two soluble LiO_2 compounds, yielding insoluble Li_2O_2 at the surface [Eq. (1)]:

$$2\,LiO_2 \rightarrow Li_2O_2 + O_2 \qquad (1)$$

In nonaqueous solvents, the one-electron O_2 reduction product is the superoxide radical anion ($O_2^{\cdot-}$), which is soluble in some solvents like DMSO and stabilized by large alkylammonium cations. In Li^+ solutions, however, LiO_2 is unstable and can undergo a second electron transfer or dismutate, forming insoluble Li_2O_2. The mechanistic pathway will depend on the experimental conditions. There has been a recent controversy about the occurrence of the disproportionation reaction based on Raman evidence of the composition of toroids formed in an aprotic Li–O_2 cell.[6]

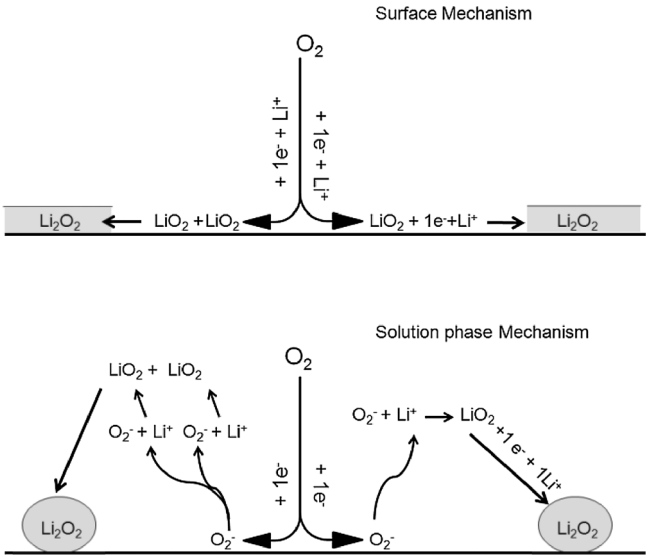

Scheme 1. Scheme of reactions for surface and solution-phase mechanisms of the ORR in lithium-containing electrolyte.

The present work focuses on the disproportionation of soluble LiO_2 into insoluble Li_2O_2 and O_2 by adding lithium ions to a tetrabutylammonium (TBA)-stabilized solution of superoxide electrogenerated by O_2 reduction at a Au surface. Quartz crystal microbalance under electrochemical control (EQCM) and atomic force microscopy (AFM) have been employed to find evidence of LiO_2 disproportionation through the potentiostatic generation of $O_2^{\cdot-}$.

The solubility of O_2 in DMSO containing lithium is 2 mM;[4a] for Li^+ concentrations above this value, that is, in 5 mM $LiPF_6$ solution, however, a new cathodic peak at 2.0–2.5 V is observed in addition to the reversible O_2/O_2^- peak (Figure 1). This is attributed to the formation of Li_2O_2 on the surface, as reported for increasing concentrations of lithium ions.[5b,7] We also noticed passivation of the surface and the disappearance of the superoxide oxidation peak in the back scan for Li^+ concentrations larger than 5 mM. During the back scan, we observe a new peak at 3 V, which corresponds to the oxidation of surface Li_2O_2, as has been demonstrated by differential electrochemical mass spectrometry[8] and Raman spectroscopy.[7] For a 5 mM lithium-ion concentration, only one reduction peak is apparent, which shifts to more positive potentials with increasing lithium concentration, as the electrochemical reduction requires Li^+ ions.[5b]

The onset of Li_2O_2 formation, according to the Raman intensity at 788 nm,[7] coincides with the peak at 2.55 V before

[a] Dr. M. del Pozo, W. R. Torres, S. E. Herrera, Prof. E. J. Calvo
Department: INQUIMAE, Facultad de Ciencias Exactas y Naturales
Pabellón 2, Ciudad Universitaria, 1428 Buenos Aires (Argentina)
E-mail: calvo@qi.fcen.uba.ar

The ORCID identification number(s) for the author(s) of this article can be found under http://dx.doi.org/10.1002/celc.201600081.

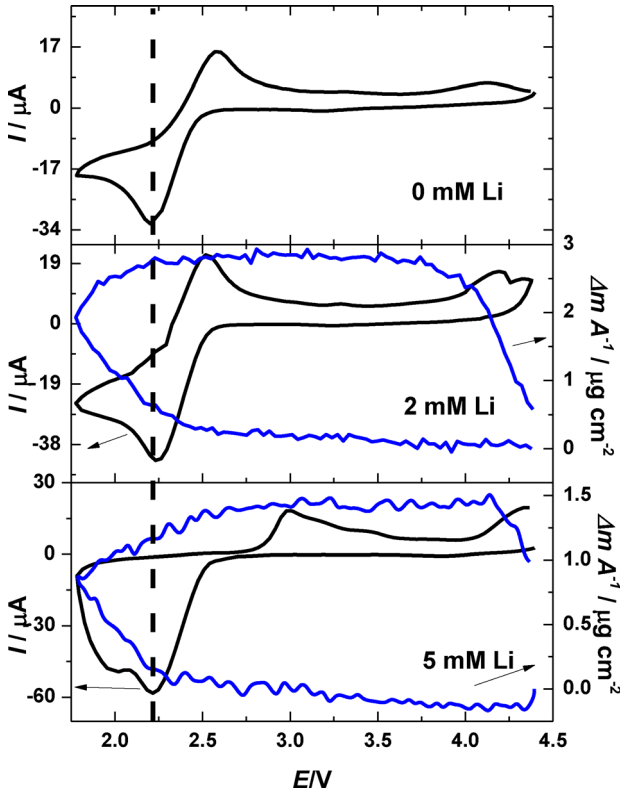

Figure 1. Cyclic voltammetry of O_2 in 0.1 M $TBAPF_6$ in DMSO (upper panel), in 2 mM $LiPF_6$ with 98 mM $TBAPF_6$ (middle panel), and in 5 mM $LiPF_6$ 95 mM $TBAPF_6$ (lower panel) on Au at 20 mV s^{-1} and simultaneous EQCM gravimetry.

reaching the second reduction peak and with the onset of a mass increase, as shown in Figure 1. Notice that the mass does not decrease above 3.5 V in spite of the Raman spectroscopic evidence of lithium peroxide decay,[7] owing to the formation of decomposition products on the surface, as revealed by XPS.[9]

Lithium peroxide can be formed by disproportionation of LiO_2 or by two consecutive one-electron and lithium-ion transfer steps to molecular oxygen [Eqs. (2) and (3)]:

$$LiO_2 + Li^+ + e^- \rightarrow Li_2O_2 \quad 3.27\,V \qquad (2)$$

$$O_2 + 2\,Li^+ + 2\,e^- \rightarrow Li_2O_2 \quad 2.96\,V \qquad (3)$$

Rotating ring-disk electrode (RRDE) experiments have shown that soluble superoxide is a stable species in TBA solutions and can be detected in the solution downstream at the ring electrode,[10] whereas Raman studies revealed the formation of Li_2O_2 in lithium-containing electrolyte.[7] A ring-current peak in the chronoamperometry during ORR at 2.0 V (shown in Figure 2) demonstrates a burst in the yield of soluble superoxide during the current decay until the surface is passivated and the disk and ring currents drop to zero.

Notice that both the disk and ring currents have a steady value after the superoxide peak, probably owing to reduction of oxygen at a partly blocked surface before full passivation of the Au surface[11] with formation of Li_2CO_3, LiF, and other sol-

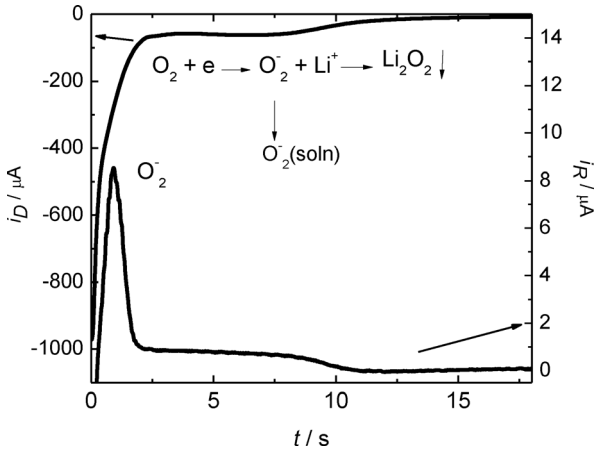

Figure 2. Chronoamperometry of the Au/Au RRDE in O_2-saturated 0.1 M $LiPF_6$/DMSO electrolyte with detection of O_2^- at the Au ring electrode. Disk electrode potential, $E_D = 2.0$ V; ring electrode potential, $E_R = 3.0$ V; $W = 9$ Hz; collection efficiency, $N_0 = 0.29$.

vent and electrolyte decomposition products at the surface, as shown by XPS.[9] A detailed RRDE study has shown that the ring-current peak has a maximum at 2.2 V, owing to the competition of superoxide formation and destruction through a second electrochemical step and disproportionation.[11]

Bruce et al. have argued that the potential of the $O_2/O_2^{-\cdot}$ peak is below the thermodynamic potential for the formation of Li_2O_2, so they speculated that spontaneous disproportionation of O_2^- to form Li_2O_2 takes place,[1c] which is in line with the mechanism proposed by Laoire et al.[4a,12] They also estimated a first-order rate constant for the dismutation of superoxide of 0.03 s^{-1} from electrochemical experiments and 0.07 s^{-1} from homogeneous experiments by using KO_2 in lithium-ion solutions.[5b] At a fast-potential sweep rate, that is, 100 mV. s^{-1}, $O_2^{-\cdot}$ disproportionation is too slow to be observed.

In contrast to the mechanism that involves superoxide disproportionation, Yu and Ye recently concluded that superoxide does not disproportionate, based on surface Raman studies of lithium superoxide and peroxide.[7] They questioned reliable experimental support for the mechanism of superoxide dismutation in the reports by Bruce et al, because all of the electrochemical experiments were under potential control.

Amin and co-workers, however, reported Raman evidence of the composition of toroids formed in an aprotic Li–O_2 cell with outer LiO_2-like and inner Li_2O_2 regions, consistent with superoxide disproportionation at the solid/solution interface.[6]

It seems that different experimental results have been reported for experiments carried out under different conditions, and one should be very careful to assess the contribution of different possible mechanism pathways for the ORR in aprotic solutions containing lithium ions.

In the present Communication, we report the effect of adding $LiPF_6$ to an O_2-saturated DMSO/TBA solution after generating stable soluble superoxide on the Au surface as the electrode open-circuit potential was followed from the O_2/O_2^- (2.65 V) to the O_2/Li_2O_2 (2.96 V) equilibria, as shown in Figure 3. Above the reversible O_2/O_2^- potential, no electroreduction of LiO_2 [Eq. (2)] is possible and any formation of Li_2O_2 on the sur-

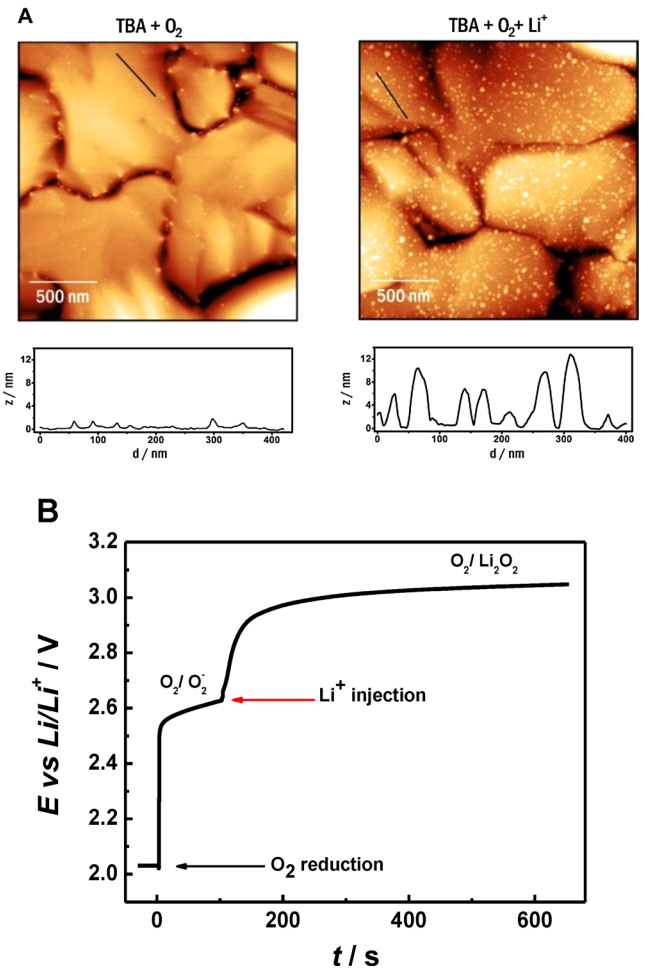

Figure 3. A) AFM images after the reduction of O_2 in $TBAPF_6$ 0.1 M in DMSO and with lithium ion addition. B) Potential monitored during experiment with lithium addition.

face most likely results from the chemical disproportionation of superoxide in the presence of lithium ions. Furthermore, in the absence of Li^+ ions after switching off the cell, the open-circuit potential reached a plateau at approximately 2.65 V and the surface was examined by using AFM. (Figure 3 A top left). Topography AFM images show no significant formation of insoluble products by dismutation of soluble O_2^- in the absence of soluble Li^+. However, in a second experiment, after reaching the open-circuit potential plateau at 2.65 V, which corresponds to O_2/O_2^- (Figure 3 B), 0.1 M $LiPF_6$ was added to reach a final concentration 10 mM. This resulted in an increase of the open-circuit potential to a value close to 3 V, as a result of the Li_2O_2/O_2 surface reaction. After rinsing with solvent, the surface was examined again through AFM, and Figure 3 A right shows a homogeneous deposit of 10–14 nm nanoparticles on the Au surface. Under similar conditions, Yu and Ye[7] found a Raman signal at 788 cm^{-1}, owing to the O–O stretching of Li_2O_2 for only a 2 mM lithium-ion concentration. The morphology and height of the Li_2O_2 deposit is similar to that reported by direct O_2 electroreduction in DMSO containing Li^+.[1c,13] The nanoparticles at the Au surface resulted from the electrogenerated O_2^- in the solution adjacent to the electrode and the lithium ions added to the electrolyte. We take this as strong evidence for

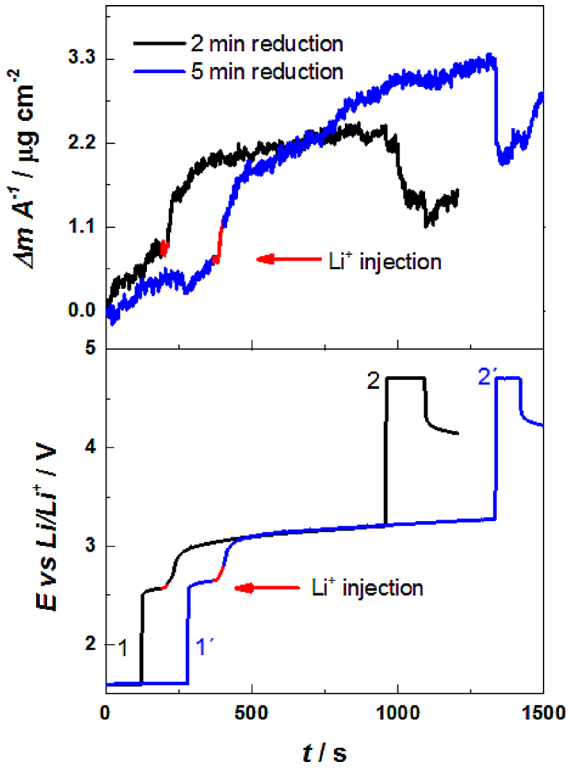

Figure 4. $\Delta m A^{-1}$ and electrode potential, *E*, as a function of time during the EQCM experiment. Arrows indicate the injection of lithium solution.

the homogeneous dismutation of soluble lithium superoxide into insoluble Li_2O_2 at the Au surface.

Further evidence was obtained with EQCM in a similar experiment, where a 1.6 V potential was applied for a few minutes to generate O_2^- in the solution adjacent to the Au-coated quartz crystal (see Figure 4 1 and 1′), and the gravimetric mass density ($\Delta m A^{-1}$) value remains practically constant during the potentiostatic pulse.

After injection of 0.1 M $LiPF_6$, $\Delta m A^{-1}$ increases and reaches 2.2 µg cm^{-2}, which is interpreted as the deposition of Li_2O_2 onto the surface, and the open-circuit potential evolves to a value close to 3 V (Li_2O_2/O_2 equilibrium potential). The open-circuit potential follows the same behavior as that registered in the AFM experiment and, regardless of the superoxide generation time, the open-circuit potential evolves to practically the same value after lithium injection.

Finally, the electrode was oxidized (Figure 4 2 and 2′) in order to dissolve the lithium peroxide formed on the surface. A pronounced decrease in the gravimetric mass is observed, but the initial mass cannot be recovered by electrochemical oxidation.

Both the nanoparticle deposit seen with AFM as well as the change in open-circuit potential and the gravimetric mass confirm, for the first time, that LiO_2 disproportionation takes place in solution near the Au electrode after adding lithium ions to the electrochemically generated superoxide ion. In this experiment, a two-electron transfer to oxygen to form Li_2O_2 is precluded, as the electrode potential was always more positive than 3 V.

Surface superoxide dismutation does not require two adjacent O_2^- molecules, because electrons are mobile at the underlying Au electrode, unlike bimolecular collision dismutation of soluble superoxide with a first-order rate constant for O_2^- in DMSO of 0.07 s^{-1}.[11]

Therefore, it is more likely that, upon addition of lithium ions, adsorbed superoxide dismutates to yield insoluble Li_2O_2 and release oxygen.

In summary, this work has demonstrated, for the first time, the dismutation of electrochemically generated TBA-stabilized superoxide in DMSO by injecting 0.1 M $LiPF_6$ to yield Li_2O_2 nanoparticles on the surface with the release of O_2. Although the experimental design excludes the possibility of two heterogeneous one-electron transfers to oxygen, EQCM and AFM results show the evolution of stable $O_2^-TBA^+$ into unstable LiO_2, which undergoes homogeneous disproportionation with further deposition on suitable surface sites.

Experimental Section

Anhydrous dimethyl sulfoxide (DMSO, ≥99.9%; Sigma–Aldrich), lithium hexafluorophosphate ($LiPF_6$, battery grade, ≥99.99%, trace metals basis; Sigma–Aldrich), and tetrabutylammonium hexafluorophosphate ($TBAPF_6$, ≥99.99%; Sigma–Aldrich), Li wire (99.9%, trace metals basis; Aldrich) were stored in the argon-filled MBRAUN glove box with an oxygen content ≤ 0.1 ppm and water content below 1.4 ppm. All solutions were prepared inside of the glove box and the water content was measured by using a Karl Fisher 831 KF coulometer (Metrohm).

EQMC has been described elsewhere.[10] The Au-coated crystal was mounted in the EQCM cell by means of O-ring seals with only one face in contact with the electrolyte; this electrode was a common ground to both the ac and dc circuits. The reference electrode was a Pt wire coated with $LiMn_2O_4/Li_2Mn_2O_4$ inside of a capillary with 1 M $LiPF_6$ in DMSO. This reference electrode was calibrated with respect to the Li/Li^+ couple inside the argon glove box (3.7 V vs. Li/Li+). All of the potentials herein are referred to the Li/Li^+ sytem. A Pt gauze (Good-fellow PT008710/43) was used as the auxiliary electrode.

For ex situ AFM experiments, a three-electrode EC–AFM electrochemical cell was built using Teflon® and a Kalrez O-ring pressed onto a gold sample with a 0.64 cm^2 area. A $LiMn_2O_4/Li_2Mn_2O_4$-coated platinum wire was used as the reference electrode and a platinum coil as the counter electrode. The cell was contained in a glass cylinder environmental chamber filled with dry oxygen. The experiments were carried out with a potentiostat/galvanostat connected to the AFM (EC–AFM, Agilent 5500 AFM/SPM). The surface was scanned by using AFM with an insulating triangular Si tip PointProbe® Plus NCL non-contact/soft tapping mode (radius <10 nm force constant 48 N m^{-1}, resonance frequency 157.85 kHz) using tapping mode. Image analysis was performed with Gwyddion 2.33 software (http://hwyd dion.net/).

The main experiment was chronoamperometry performed at 1.6 V for 2 or 5 min in 0.1 M $TBAPF_6$ in DMSO. After this time, the system was registered at the open-circuit potential and then a few milliliters of 0.1 M $LiPF_6$ were added to the cell. In the case of the EQCM experiment, the evolution of the potential and the change of gravimetric mass were registered simultaneously for 15 min. After this time, a potential of 4.7 V was applied with the aim of oxidize the surface products. In AFM measurements, after adding the lithium solution, the open-circuit potential was monitored for 15 min. After this time, the solution was removed and the surface was rinsed with ten aliquots of DMSO (100 μL) and dried under Ar before scanning the surface.

Acknowledgements

FS-Nano 07 funding as well as postdoctoral and doctoral research fellowships from CONICET and ANPCyT PICT 2012 No. 1452 and from ANCPCyT (M.d.P.) and from CONICET (W.R.T. and S.E.H.) are gratefully acknowledged.

Keywords: atomic force microscopy · electrochemical quartz crystal microbalance · lithium · rotating ring-disk electrode · superoxide

[1] a) K. M. Abraham, *Lithium-air and other batteries beyond lithium-ion batteries*, (Ed.: K. M. A. Bruno Scrosati, Walter van Schalkwijk, Jusef Hassoun) John Wiley & Sons, Inc2013., **2013**; b) N. B. Aetukuri, B. D. McCloskey, J. M. Garcia, L. E. Krupp, V. Viswanathan, A. C. Luntz, *Nat. Chem.* **2015**, *7*, 50–56; c) P. G. Bruce, S. A. Freunberger, L. J. Hardwick, J. M. Tarascon, *Nat. Mater.* **2012**, *11*, 172; d) S. A. Freunberger, Y. Chen, Z. Peng, J. M. Griffin, L. J. Hardwick, F. Barde, P. Novak, P. G. Bruce, *J. Am. Chem. Soc.* **2011**, *133*, 8040–8047; e) L. J. Hardwick, P. G. Bruce, *Current Opinion in Solid State and Materials Science* **2012**, *16*, 178–185.

[2] K. M. Abraham, Z. Jiang, *J. Electrochem. Soc.* **1996**, *143*, 1–5.

[3] T. Ogasawara, A. Debart, M. Holzapfel, P. Novak, P. G. Bruce, *J. Am. Chem. Soc.* **2006**, *128*, 1390–1393.

[4] a) C. O. Laoire, S. Mukerjee, K. M. Abraham, E. J. Plichta, M. A. Hendrickson, *J. Phys. Chem. C* **2010**, *114*, 9178–9186; b) B. D. McCloskey, D. S. Bethune, R. M. Shelby, G. Girishkumar, A. C. Luntz, *J. Phys. Chem. Lett.* **2011**, *2*, 1161–1166.

[5] a) B. D. Adams, C. Radtke, R. Black, M. L. Trudeau, K. Zaghib, L. F. Nazar, *Energy Environ. Sci.* **2013**, *6*, 1772–1778; b) L. Johnson, C. Li, Z. Liu, Y. Chen, S. A. Freunberger, P. C. Ashok, B. B. Praveen, K. Dholakia, J. M. Tarascon, P. G. Bruce, *Nat. Chem.* **2014**, *6*, 1091–1099; c) Z. Peng, S. A. Freunberger, L. J. Hardwick, Y. Chen, V. Giordani, F. Barde, P. Novak, D. Graham, J. M. Tarascon, P. G. Bruce, *Angew. Chem. Int. Ed.* **2011**, *50*, 6351–6355; *Angew. Chem.* **2011**, *123*, 6475–6479; d) M. J. Trahan, S. Mukerjee, E. J. Plicht, M. A. Hendrickson, K. M. Abraham, *J. Electrochem. Soc.* **2013**, *160*, A259–A267; e) N. Lopez, D. J. Graham, R. McGuire Jr, G. E. Alliger, Y. Shao-Horn, C. C. Cummins, D. G. Nocera, *Science* **2012**, *335*, 450–453; f) D. Zheng, Q. Wang, H. S. Lee, X. Q. Yang, D. Qu, *Chem. Eur. J.* **2013**, *19*, 8679–8683; g) J. Hassoun, F. Croce, M. Armand, B. Scrosati, *Angew. Chem. Int. Ed.* **2011**, *50*, 2999–3002; *Angew. Chem.* **2011**, *123*, 3055–3058; h) H. G. Jung, J. Hassoun, J. B. Park, Y. K. Sun, B. Scrosati, *Nat. Chem.* **2012**, *4*, 579–585.

[6] D. Zhai, H. H. Wang, K. C. Lau, J. Gao, P. C. Redfern, F. Kang, B. Li, E. Indacochea, U. Das, H. H. Sun, H. J. Sun, K. Amine, L. A. Curtiss, *J. Phys. Chem. Lett.* **2014**, *5*, 2705–2710.

[7] Q. Yu, S. Ye, *J. Phys. Chem. C* **2015**, *119*, 12236–12250.

[8] A. C. Luntz, B. D. McCloskey, *Chem. Rev.* **2014**, *114*, 11721–11750.

[9] F. Marchini, S. Herrera, W. Torres, A. Y. Tesio, F. J. Williams, E. J. Calvo, *Langmuir* **2015**, *31*, 9236–9245.

[10] W. R. Torres, L. Cantoni, A. Y. Tesio, M. del Pozo, E. J. Calvo, *J. Electroanal. Chem.* **2016**, *765*, 45–51.

[11] W. Torres, N. Mozhzhukhina, A. Y. Tesio, E. J. Calvo, *J. Electrochem. Soc.* **2014**, *161*, A2204–A2209.

[12] O. Laoire, S. Mukerjee, K. M. Abraham, E. J. Plichta, M. A. Hendrickson, *J. Phys. Chem. C* **2009**, *113*, 20127–20134.

[13] F. Marchini, S. E. Herrera, E. J. Calvo, F. J. Williams, *Surf. Sci.* **2016**, *646*, 154–159.

Manuscript received: February 16, 2016
Final Article published: ■■ ■■, 2016

Happy release: The dismutation of electrochemically generated tetrabutylammonium-stabilized lithium superoxide in DMSO by injecting 0.1 M $LiPF_6$ is shown to yield Li_2O_2 nanoparticles on the surface with release of O_2.

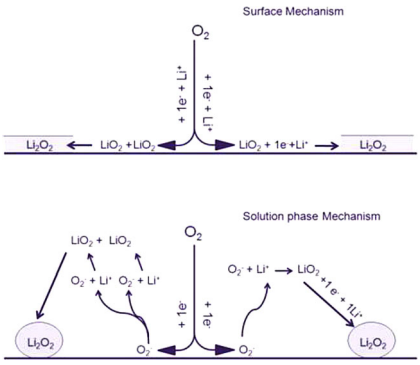

*M. del Pozo, W. R. Torres, S. E. Herrera, E. J. Calvo**

■■ – ■■

New Evidence of LiO_2 Dismutation in Lithium–Air Battery Cathodes